Flexible Capacitive Tactile Sensor Based on Micropatterned Dielectric Layer

*Tie Li, Hui Luo, Lin Qin, Xuewen Wang, Zuoping Xiong, Haiyan Ding, Yang Gu, Zheng Liu, and Ting Zhang**

***F**lexible tactile sensors are considered as an effective way to realize the sense of touch, which can perform the synchronized interactions with surrounding environment. Here, the utilization of bionic microstructures on natural lotus leaves is demonstrated to design and fabricate new-type of high-performance flexible capacitive tactile sensors. Taking advantage of unique surface micropattern of lotus leave as the template for electrodes and using polystyrene microspheres as the dielectric layer, the proposed devices present stable and high sensing performance, such as high sensitivity (0.815 kPa^{-1}), wide dynamic response range (from 0 to 50 N), and fast response time (≈38 ms). In addition, the flexible capacitive sensor is not only applicable to pressure (touch of a single hair), but also to bending and stretching forces. The results indicate that the proposed capacitive tactile sensor is a promising candidate for the future applications in electronic skins, wearable robotics, and biomedical devices.*

1. Introduction

Wearable electronic devices are becoming more and more popular these days, and lots of efforts have been devoted toward realization of highly sensitive and flexible sensors.[1] Among them, the flexible/stretchable tactile devices, which can be integrated in the curved surfaces such as touchscreen, flexible displays and even human body, have received considerable attention due to their potential applications in robotics, prosthetics and other wearable systems.[2] These flexible sensors could help the electronic devices understand how real-world objects "feel" during interactions, also obtain biosignals such as finger touching and body motions.[3,4] Since the early researches of field-effect transistor (FET) based flexible tactile sensors or "electronic-skins" were reported by Someya et al.,[5,6] great progress has been made in the design of such "skin-like" tactile sensors.[7–10] For example, Yun et al. reported a polymer-waveguide-based flexible tactile sensor array for dynamic response with high sensitivity (16% N^{-1}), and high bendability in response to dynamic input force (0–3 N) without electronic components.[7] Gerratt et al. have reported an elastomeric electronic skin designed to be worn over the hand for prosthetic tactile sensation to monitor real-time finger movement and register distributed pressure along the entire length of the finger.[9] Yao et al. presented a wearable sensors based on stretchable Ag nanowire conductors, which enable the detection of the strain (up to 50%) and pressure (up to 1.2 MPa) with fast response time (40 ms).[10] Nevertheless, most of those were not widely adopted because of certain drawbacks such as wide detection range but suffering from slow response time; great sensitivity but limited by complicated preparation method. Hence, the tactile sensors with facile fabrication techniques and possessing comprehensive properties of high sensitivity, fast response time, low power consumption, and high stability are required for their specific applications.

Various technical approaches to satisfy these practical requirements have been investigated in the last few years.[11] In general, there are mainly three different configurations of tactile sensing technology that have been proposed and

Dr. T. Li, H. Luo, L. Qin, X. W. Wang, Z. P. Xiong, H. Y. Ding, Y. Gu, Prof. T. Zhang
i-Lab
Suzhou Institute of Nano-Tech and Nano-Bionics
Chinese Academy of Sciences
398 Ruoshui Road, Suzhou 215123, P. R. China
E-mail: tzhang2009@sinano.ac.cn
X. W. Wang, Prof. Z. Liu
School of Materials Science and Engineering
Nanyang Technological University
50 Nanyang Avenue 639798, Singapore

DOI: 10.1002/smll.201600760

www.MaterialsViews.com

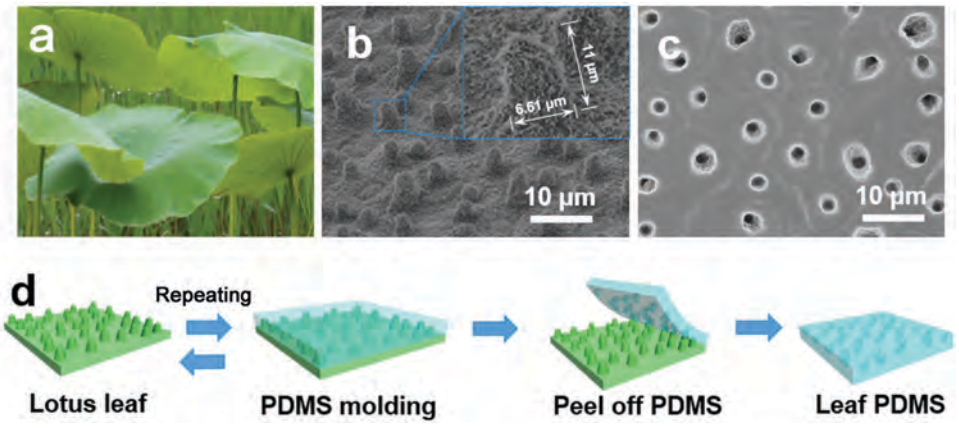

Figure 1. a,b) The photo image and 45° view SEM images of a lotus leaf. c) Typical top view SEM image of micropatterned PDMS film. d) Schematic of the fabrication process for micropatterned PDMS film.

demonstrated: (i) FET. Inorganic nanowires and conducting polymers, including Si nanowires, carbon nanotubes, and polypyrrole (PPy) microspheres, have been employed for constructing flexible FETs-based tactile sensors. These materials serve as electrodes and sensing materials due to their great electrical and mechanical properties, however, the fabrication of these sensors is usually based on the complex and expensive micro-electro-mechanical system (MEMS) process, which is difficult to realize industrialization.[12–16] (ii) piezoresistor. The piezoresistive effect has been demonstrated using flexible piezoelectrical materials with microstructured/patterned electrodes.[17] For example, as a typical piezoelectrical material, ZnO was widely investigated for construction of flexible pressure sensors due to their high piezoelectric constant, especially for hexagonal structure of ZnO nanowires.[18–21] However, the flexibility of these inorganic piezoelectrical materials is not comparable to that of organic materials and polymers, which limits their applications by the small dynamic response range. (iii) capacitor. For capacitive devices, Au film, carbon nanotubes, and Ag nanowire networks embedded in polydimethylsiloxane (PDMS) have been developed in construction of flexible devices as the top and bottom electrodes.[22] The microstructured/patterned dielectric layer (e.g., pyramid and line architecture) of capacitive sensors has been proven to give high sensitivity and fast response time.[23] The high sensitivity is mainly contributed by the gas phase existing in micropatterned dielectric layer, which can easily produce deformation when the tiny force applied to the device. However, such design carry inherent drawbacks such as the gas phase in dielectric layers brings erratic baseline, hysteresis, and irreproducible sensitivity. Hence, it is still a challenge to develop a high-sensitivity flexible tactile sensor using a low-cost, facile but efficient prepared strategy, especially for the microstructured/patterned dielectric layer.

An effective approach toward improving the performances of tactile sensors is the judicious selection of patterned electrode. Inspired from the bionic inspired fabrication strategy, the micro/nanostructures of natural plants can be used as an effective soft mold to fabricate the micropatterned electrodes.[24] In particular, Su et al. reported a new bioinspired strategy by mimosa leaf to fabricate flexible pressure sensors with touch sensitivity, however, it was restricted by the relatively narrow detection range of 0–1.5 kPa.[25] Here, we report a novel flexible capacitive tactile sensor based on micropatterned flexible substrate duplicated from the lotus leaf, which possesses uniform surface microstructures and is easy to obtain as well as duplicate. The device was constructed by the micropatterned top and bottom electrodes coupled with polystyrene (PS) microspheres as the dielectric layer. The performance test indicated that the sensitivity of this tactile sensor can be tuned by adjusting the diameters of PS microspheres and lotus leaves. The results shows that when the diameter of PS is 670 nm and the average diameter of microstructures is 6.61 ± 1.06 μm and the height is 11 ± 0.93 μm, the optimum sensitivity (0.815 kPa^{-1}) can be obtained with a short response time (≈38 ms) and low detection limit (17.5 Pa). Benefiting from those above, this microstructured sensor array we proposed present sensitive and fast response to bending, stretching force, and pressure. Such high sensing performance makes the flexible capacitive tactile sensor as the promising candidate for various applications such as in artificial electronic-skins and wearable electronics.

2. Results and Discussion

The fabrication of flexible micropatterned PDMS substrates is accomplished with the lotus leaf serving as the soft mold. From the scanning electron microscopy (SEM) observation of a lotus leaf in **Figure 1**a,b, a regular microcylinder pattern with an average diameter of 6.61 ± 1.06 μm and height of 11 ± 0.93 μm can be found on the leaf surface, which provides a unique and inexpensive molding template to fabricate micropatterned PDMS film. It is worth noticing that the morphology of this microcylinder did not change as fresh or dry specimen, which was proven by the SEM images of the same lotus leaf before and after drying as shown in Figure S1a,b of the Supporting Information. After replicating process, the typical morphology of the microstructured PDMS film substrate was characterized by top-view SEM, and the results indicate that uniform caves were formed by replication of microstructures from the lotus leaf mold (Figure 1c) and the cave was unblocked by the PDMS (Figure S1c, Supporting

DOI: 10.1002/smll.201600760

Information). Even the small embossment on lotus leaf can also be duplicated successfully as coarse groove scattered on the surface of the cave appeared in Figure S1c of the Supporting Information. Furthermore, one mold can be reused several times and the resulting films were characterized as shown in Figure S2 of the Supporting Information. It shows that the prepared films were mainly alike in morphology, structure and quantity of all duplicated caves, and even a tiny detailed structure at same position was uniformly obtained (marked in Figure S2c,d, Supporting Information), indicating that the repeatedly operations did not affect the consistency of those microstructured PDMS substrates. As previous reported, though several microstructural templates such as pyramid-shaped microstructures on top of Si have been used to construct flexible substrates for flexible electronic sensors,[22–25] the complicated MEMS fabricating process must be employed to prepare the Si mold. In comparison, the novel natural template and duplicating method in this work can also obtain the same effect but without the expensive and complicated instruments, and this strategy can also apply to other natural templates.

Figure 2a presents the schematic of the flexible capacitive tactile sensor based on the micropatterned PDMS/Au substrates, and Figure 2b shows the photograph of the 4 × 4 sensor matrix with the area of each individual sensor is 0.8 × 0.8 cm^2. Unlike conventional capacitive pressure sensors, this novel tactile sensor is a type of parallel plate capacitor which consists of two micropatterned PDMS/Au flexible substrates as plate electrodes and PS microsphere as middle dielectric layer. The SEM images (Figure 2c,d) of the PS microspheres indicate their good uniformity with the average diameter of each PS microsphere of 670 nm. This size is smaller than that of caves in micropatterned PDMS/Au substrate, so that the PS microspheres in dielectric layer can easily drop into those microcaves during spin-coating, as proven in Figure S1d of the Supporting Information. And to investigate the reproducible preparation of PS based dielectric layers, the equivalent mass of PS microspheres were spined onto above mentioned films with geometric identity from one mold and then the cross-sections of samples were examined as shown in Figure S3 of the Supporting Information, revealing the similar thickness of those as-prepared dielectric layers (7.86, 7.86, 7.78, and 7.84 μm), which is beneficial to obtain the consistent initial capacitance values (≈14 pF) of sensors under same preparation process. The key innovation of our design is to improve the sensitivity and response range by controlling the dynamic change of the dielectric layer, which can be contributed by an enhanced porosity and surface area of micropatterned PDMS stemmed from the pattern of lotus leaf. As known that the capacitance value of parallel plate capacitor $C = (\varepsilon \cdot S)/d$, where ε is the dielectric constant, S is the relative plate area, and d is the plate distance. As

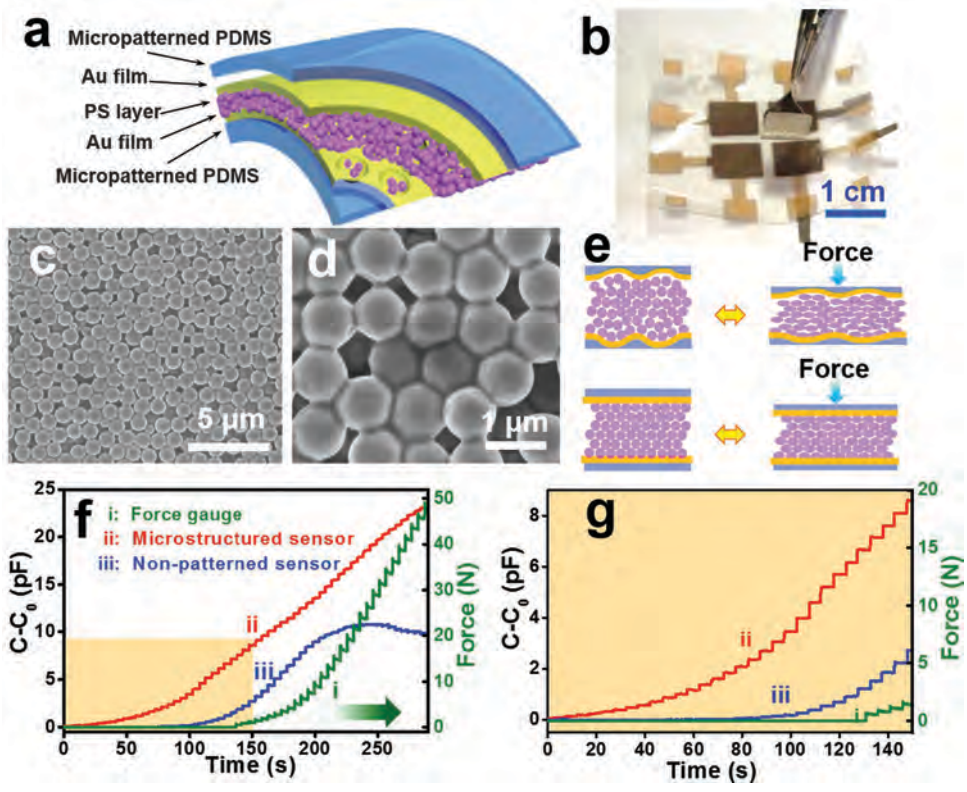

Figure 2. a) The schematic of flexible capacitive tactile sensor. b) The photo image of 4 × 4 capacitive tactile sensor matrix and the dimension of each individual sensor is 0.8 × 0.8 cm^2. c,d) The low and high amplification SEM images of PS microspheres. e) Schematic representation for the deformation of capacitive tactile sensors with and without micropatterned PDMS/Au electrodes. f) Real-time capacitance response curves with stepwise applied forces of microstructured sensor, nonpatterned sensor, and commercial force gauge. g) Amplified response curves of shadow area in (f). The applied forces did not display in (f) until 130 s due to the intrinsic feedback measuring accuracy (lowest to 0.2 N) of this commercial force gauge.

DOI: 10.1002/smll.201600760

illustrated in Figure 2e, when an external pressure is applied, the microcaves existing in flexible substrates will be extended resulting in an enlarged relative plate area (S). Combined with the reduced distance (d) caused by pressure, it will lead to large capacitance (C) change of the sensors. And more, the PS microspheres extruded from microcave will take part in the rearrangement of dielectric materials and further enhance the capacitance change, which can be seen from the morphology changes with applied external pressure as shown in Figure S4 of the Supporting Information, demonstrating that the PS balls are filling the space normally taken by air after compression. Correspondingly, the device based on nonpatterned PDMS films is difficult to enhance the capacitance through geometrical structure and extra rearrangement except the distance (d) change.

Upon above analysis, we compared the performance of the capacitive tactile sensors constructed by PS microsphere dielectric layer with and without micropatterned PDMS/Au electrodes, which are defined as microstructured sensor and nonpatterned sensor. Their initial capacitance values were 14 pF and 10 pF measured by the Capacitance Meter (Agilent E4981A), respectively. As shown in Figure S5 of the Supporting Information, the thicknesses of the PS dielectric layer with and without micropatterned electrodes were 7.89 and 8.23 μm, respectively, under the same preparation conditions, which was caused by that PS microspheres in dielectric layer can easily drop into those microcaves during spining. And according the above formula mode of capacitance value (C), the reduced distance (d) will result in the large C value. Here, the plate distance (it is about twice of the PS layer thickness because the device was assembled by face to face) of microstructured sensor is less than that of nonpatterned sensor, hence it inevitably possesses larger initial capacitance value. Then, the commercial force gauge (Aliyiqi HF-2N) was used as standard reference sensor to establish the relationship between the applied force and the real-time capacitance changes of the tactile sensors as shown in Figure 2f. The capacitances of both sensors increase when applied force is stepwise added in the first stage. However, along with the applied force increases up to about 21 N, the capacitance of nonpatterned sensor reaches its saturation state and slightly decreases to 20 N with continuous adding the force, while the microstructured sensor presents a larger dynamic response range with no sign of saturation within the force of 0 to 50 N. Figure 2g represents the detailed information from the shadow area of Figure 2f, showing the capacitance responses of both sensors in the range of 0–20 N. Small applied forces did not display in the figure until 130 s due to the intrinsic feedback measuring accuracy (lowest to 0.2 N) of this commercial force gauge employed for large pressure range of 0–50 N. A high-precision force gauge was used to detect the tiny pressure range of 0–0.15 N and the record was displayed in Figure S6a of the Supporting Information, showing the detection limit as low as 1.12 mN, which directly demonstrates its excellent dynamic response of the microstructured sensor used to calculate the low pressure sensitivity values. These results demonstrate that the sensitivities and response ranges of the flexible capacitive sensors can be significantly improved by the unique design of the micropatterned PDMS/Au electrodes. That is because, as above described, the flexible substrate of micropatterned sensor can obtain bigger change caused by not just the normal deformation of flexible PDMS but also the expansion of vast caves when a pressure applied, resulting in generating extra working area and dielectric material coming out from the caves and taking part in capacitance behavior compared with that of nonpatterned sensor. And it is obvious that the deformability of the flexible PDMS without micropatterned is relatively constant and quite smaller than that with micropatterned when the size of sensor is fixed, directly leading to the response range is evidently improved by employing the microstructure.

The sensing performance of capacitive tactile sensors has been analyzed and the results are shown in **Figure 3**. The sensitivity is defined as $S = (\triangle C/C_0)/P$, where $\triangle C$ is the variation of capacitance ($C–C_0$), P presents applied pressure: F/A (F is the force applied on top of the tactile sensing element and A is the area of the top-bottom Au electrodes).[5] As shown in Figure 3a, two linear regions of relationship are observed between sensitivity and applied pressure. For the microstructured sensors, the high sensitivity value of 0.815 kPa^{-1} was observed at the small pressure range, which is higher than that reported in previous studies.[26–28] Although the sensitivity decreases slightly with the increase of pressure, the value (0.0047 kPa^{-1}) was also comparable to some reported capacitive tactile sensors.[27,28] Similarly, the nonpatterned sensor presents a sensitivity of 0.038 kPa^{-1} at very low forces and down to 0.002 kPa^{-1} with the increase of pressure. For evaluating the reproducibility of as-prepared flexible sensors, we investigated real-time responses of device with quickly loading/unloading pressures of 0.2, 8, and 80 kPa for five circles and low pressures of 20 and 100 Pa, respectively (Figure 3b,c). The results show that microstructured sensors present stable sensing performance with high sensitivity and great reproducibility. And more, to characterize the minimum press response and response time of microstructured sensors relevant to "tactile" application, the limits of detection was evaluated and shown in Figure S6 of the Supporting Information. Clearly, a minimum detection limit (17.5 Pa) and short response time (≈38 ms) were obtained, showing its excellent sensitivity is fit for the application of microforce sensing like "tactile" condition. Compared with previous reports displayed in Figure 3d and **Table 1**, this microstructured sensor we proposed has better sensitivity and low detection limit.[5,9,16,25–31]

The dimensional statistical results of the holes from leaf to leaf have been calculated and the effect of height and diameter to sensitivity was studied as shown in Figure S7 of the Supporting Information. It is observed that the average distribution of height and diameter of four lotus leaves are different (Figure S7a, Supporting Information). Figure S7b of the Supporting Information shows that the sensitivity can be controlled by selecting suitable leaf templates, and the cave with a mean diameter of 6.51 μm and height of 10.34 μm exhibits the best sensitivity. In addition, the effect of the PS microsphere sizes to the sensitivity of sensor was investigated as shown in Figure S8 of the Supporting Information. It can be seen that the sensitivity is also affected by the diameters of PS microspheres, which the highest sensitivity was achieved

DOI: 10.1002/smll.201600760

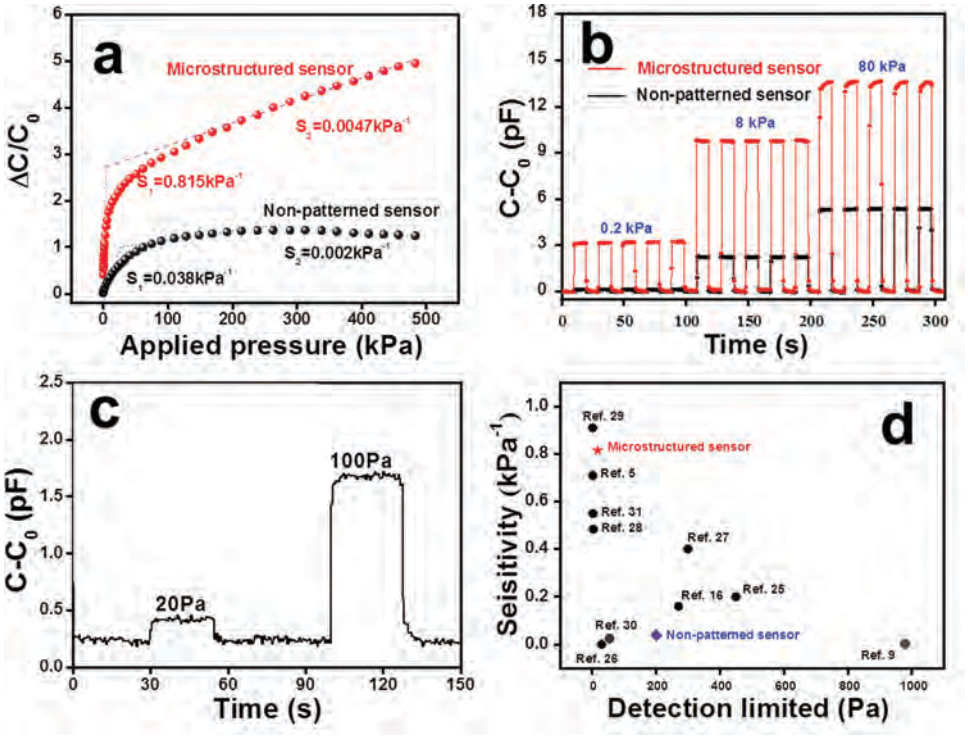

Figure 3. a) Sensitivities of micropatterned capacitance sensor (red) and nonpatterned sensor (black). b,c) The both type of tactile sensors repeated real-time responses to pressure of 0.2, 8, 80 kPa, and low 20, 100 Pa, respectively. d) Sensitivities of both type of sensors comparison with previous research results.

when the diameter is about 670 nm as above ascribed (0.282 and 0.0038 kPa^{-1} for 500 nm; 0.0023 kPa^{-1} for 800 nm). The capacitance behaviors of the devices were determined partly by the PS dielectric layer, in which the thickness and extruded activity affect the initial capacitance value and the sensitivity of flexible sensors, respectively. As shown in the SEM images of PS layers (Figure S9, Supporting Information), it can be seen that the configuration, microcaves and thickness of the flexible devices were influenced by the dimensions of PS microspheres. In the PS dielectric layers, the homogeneous distribution of the 670 nm PS microspheres were observed, yet a mass of aggregation generated with the 500 nm PS microspheres and lots of redundant uncovered sites appeared with the 800 nm PS microspheres, resulting in the more difficult dynamic rearrangement and movement caused by the applied pressure.

Table 1. The comparison of the state-of-the-art pressure response between this work and previous reported capacitive sensors.

Sensitivity [kPa^{-1}]	Detection limit [Pa]	Reference
0.710	2.5	[5]
0.024	980	[9]
0.160	270	[16]
0.200	450	[25]
7.1×10^{-4}	30	[26]
0.400	300	[27]
0.484	4.13	[28]
0.910	2	[29]
0.023	56	[30]
0.550	3	[31]
0.815	17.5	This work

Besides response to pressure, the flexible capacitive sensors also show the capability to detect the bending and stretching forces with different response patterns. As shown in **Figure 4**, the stretching (33% deformation, holding 10 s), bending (120°, holding 10 s), and pressure touching by a single hair (about 18, 26, and 95 Pa) are repeatedly applied to the flexible device for several times. The real-time $\triangle C(C–C_0)–t$ curves were measured and displayed in Figure 4a–c, respectively. Remarkably, the flexible capacitive sensors show the distinct pattern responses to different type of forces (bending, stretching, and pressure touching by a single hair). In addition, to understand the pressure produced by hair, a section SEM image of a single hair is characterized as shown in Figure S10 of the Supporting Information. It can be seen that the surface area is about 5.8×10^{-9} m^2, which is so small that a very light hair will produce a sufficient pressure to cause the device response. Moreover, pressure touching in Figure 4c is main caused by slight hand pushing and conducted to the surface of the tactile sensor through a single hair. Furtherly, combining with the appropriate pattern recognition analysis of different shapes of $\triangle C–t$ curves, these three different forces can be distinguished. These results suggest the flexible capacitive sensing devices can be used in monitoring the strain and the friction force, which is very promising for the smart robotic systems.

DOI: 10.1002/smll.201600760

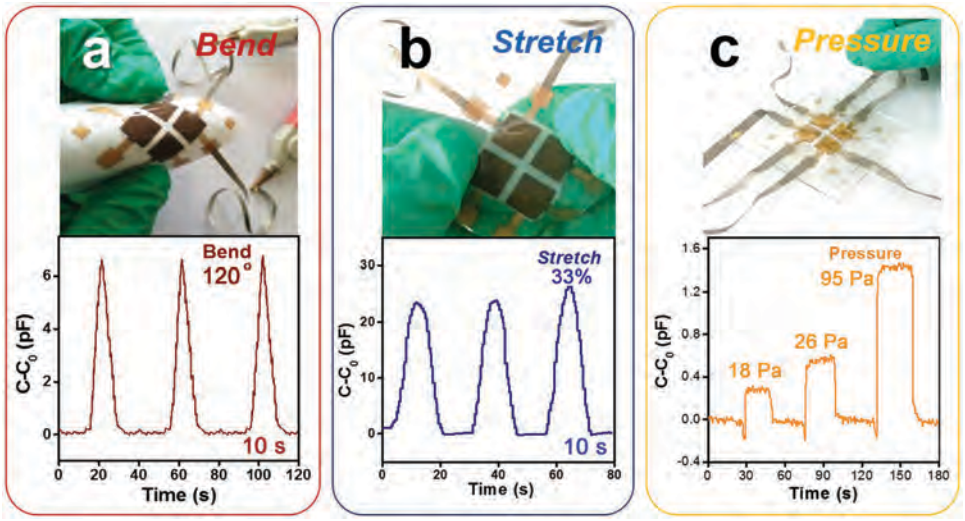

Figure 4. a) Bending force (120°, 10 s), b) stretching force (33%, 10 s), and c) pressure touching by a hair (about 18, 26, and 95 Pa) were applied to a flexible capacitive tactile sensor.

3. Conclusion

In summary, we proposed a flexible capacitive tactile sensor using microstructured PDMS/Au electrodes and PS microsphere dielectric layer. The lotus leaves served as the unique cost-effective molding templates to fabricate uniform microcave patterned PDMS film. These flexible capacitive devices show high sensitivity (0.815 kPa^{-1}), large dynamic response range (from 0 to 50 N), and fast response time (≈38 ms). The microcaves in PDMS/Au electrode play an essential role to rearrange the PS microspheres in dielectric layer upon applying external pressure, and eventually endow the flexible device with high sensitivity and reproducibility. In addition, our device also shows the great capability in detection of bending and stretching forces, which is significant for the future electronic skins applying in smart robotic systems.

4. Experimental Section

Fabrication of Flexible Micropatterned PDMS Substrates: The fabrication process is illustrated in Figure 1d. First, PDMS prepolymer was prepared by thoroughly mixing the curing agent with the base monomer (Dow Corning Sylgard 184; the weight ratio of base to cross linker was 10:1). After degasification in vacuum for 10 min to get rid of gas bubbles at room temperature, the PDMS mixture was spin coated (at 400 rpm) onto a piece of precleaned lotus leaf (4 × 4 cm^2), and completely cured at 70 °C for 2 h. Finally, the PDMS film was peeled off from the lotus leaf template with delicate microcaves pattern. By contrast, the fabrication method of flexible *nonpatterned PDMS substrate* was the same as above description except the PDMS mixture was spin coated onto a smooth glass.

Design and Fabrication of Flexible Tactile Sensors: The schematic design of the capacitive microstructured tactile sensor based on the principle of parallel plate capacitor is shown in Figure 2a, which is constructed with two bottom and top micropatterned PDMS/Au substrates covered with Au as plate electrodes and PS microsphere as middle dielectric layer. The fabrication process includes following steps: First, the bottom and top Au electrode layers were fabricated by sputtering 120 nm Au nanoparticle through a shadow mask onto the surface of micropatterned PDMS substrates (0.8 cm length × 0.8 cm height × 0.01 cm thickness), respectively. Then, the middle dielectric layer was formed by spin coating the PS microspheres upon the as-prepared bottom and top Au electrodes (at 200 rpm). Finally, the device was face-to face assembled by the bottom and top micropatterned electrodes. Similarly, the fabrication of the nonpatterned sensor was almost same with that of above microstructured sensor except using nonpatterned PDMS substrates. For comparison, the dimensions of these kinds of tactile sensors were designed uniformly as 0.8 × 0.8 cm^2 and the amount of PS microsphere was also gone all the way.

Electrical Measurements and Testing of Flexible Tactile Sensors: The electrical characterization of each flexible tactile sensor was measured with a LCR meter (Agilent E4980A) under the signal of 1 V at 10 MHz. A force gauge (Handpi Digital force gauge, HP2) and a computer controlled movable stage (Beiguang SC movable stage) were used to measure the applied force and the displacement, respectively. All the measurements were performed under ambient conditions.

Supporting Information

Supporting Information is available from the Wiley Online Library or from the author.

Acknowledgements

T.L. and H.L. contributed equally to this work. The authors acknowledge the funding support from the National Program on Key Basic Research Project (973 Program, Grant No.2015CB351901), Strategic Priority Research Program of the Chinese Academy of Sciences (Grant No. XDA09020201), the National Natural Science Foundation of China (91123034, 61574163), the China

DOI: 10.1002/smll.201600760

Postdoctoral Science Foundation (2015M571837), and the Foundation Research Project of Jiangsu Province (BK20150364).

[1] R. A. Brooks, *Artif. Intell.* **1991**, *47*, 139.
[2] V. Maheshwari, R. F. Saraf, *Angew. Chem. Int. Ed.* **2008**, *47*, 7808.
[3] A. N. Sokolov, B. C. K. Tee, C. J. Bettinger, J. B. H. Tok, Z. N. Bao, *Acc. Chem. Res.* **2011**, *45*, 361.
[4] M. L. Hammock, A. Chortos, B. C. K. Tee, J. B. H. Tok, Z. A. Bao, *Adv. Mater.* **2013**, *25*, 5997.
[5] T. Someya, T. Sekitani, S. Iba, Y. Kato, H. Kawaguchi, T. Sakurai, *P. Natl. Acad. Sci. USA* **2004**, *101*, 9966.
[6] T. Someya, Y. Kato, T. Sekitani, S. Iba, Y. Noguchi, Y. Murase, H. Kawaguchi, T. Sakurai, *P. Natl. Acad. Sci. USA* **2005**, *102*, 12321.
[7] S. Yun, S. Park, B. Park, Y. Kim, S. K. Park, S. Nam, K. U. Kyung, *Adv. Mater.* **2014**, *26*, 4474.
[8] A. P. Gerratt, H. O. Michaud, S. P. Lacour, *Adv. Funct. Mater.* **2015**, *25*, 2287.
[9] B. W. Zhu, Z. Q. Niu, H. Wang, W. R. Leow, H. Wang, Y. G. Li, L. Y. Zheng, J. Wei, F. W. Huo, X. D. Chen, *Small* **2014**, *10*, 3625.
[10] S. S. Yao, Y. Zhu, *Nanoscale* **2014**, *6*, 2345.
[11] S. Park, H. Kim, M. Vosgueritchian, S. Cheon, H. Kim, J. H. Koo, T. R. Kim, S. Lee, G. Schwartz, H. Chang, Z. A. Bao, *Adv. Mater.* **2014**, *26*, 7324.
[12] M. Kaltenbrunner, T. Sekitani, J. Reeder, T. Yokota, K. Kuribara, T. Tokuhara, M. Drack, R. Schwodiauer, I. Graz, S. Bauer-Gogonea, S. Bauer, T. Someya, *Nature* **2013**, *499*, 458.
[13] D. J. Lipomi, M. Vosgueritchian, B. C. K. Tee, S. L. Hellstrom, J. A. Lee, C. H. Fox, Z. N. Bao, *Nat. Nanotechnol.* **2011**, *6*, 788.
[14] K. Takei, T. Takahashi, J. C. Ho, H. Ko, A. G. Gillies, P. W. Leu, R. S. Fearing, A. Javey, *Nat. Mater.* **2010**, *9*, 821.
[15] C. Pang, G. Y. Lee, T. I. Kim, S. M. Kim, H. N. Kim, S. H. Ahn, K. Y. Suh, *Nat. Mater.* **2012**, *11*, 795.
[16] L. J. Pan, A. Chortos, G. H. Yu, Y. Q. Wang, S. Isaacson, R. Allen, Y. Shi, R. Dauskardt, Z. N. Bao, *Nat. Commun.* **2014**, *5*, 3002.
[17] M. Y. Cheng, C. L. Lin, Y. T. Lai, Y. J. Yang, *Sensors* **2010**, *10*, 10211.
[18] W. Z. Wu, X. N. Wen, Z. L. Wang, *Science* **2013**, *340*, 952.
[19] C. F. Pan, L. Dong, G. Zhu, S. M. Niu, R. M. Yu, Q. Yang, Y. Liu, Z. L. Wang, *Nat. Photonics* **2013**, *7*, 752.
[20] S. N. Cha, J. S. Seo, S. M. Kim, H. J. Kim, Y. J. Park, S. W. Kim, J. M. Kim, *Adv. Mater.* **2010**, *22*, 4726.
[21] S. Xu, Y. Qin, C. Xu, Y. G. Wei, R. S. Yang, Z. L. Wang, *Nat. Nanotechnol.* **2010**, *5*, 366.
[22] H. Vandeparre, D. Watson, S. P. Lacour, *Appl. Phys. Lett.* **2013**, *103*, 204103.
[23] B. C. K. Tee, A. Chortos, R. R. Dunn, G. Schwartz, E. Eason, Z. A. Bao, *Adv. Funct. Mater.* **2014**, *24*, 5427.
[24] M. L. Seol, J. H. Woo, D. Lee, H. Im, J. Hur, Y. K. Choi, *Small* **2014**, *10*, 3887.
[25] B. Su, S. Gong, Z. Ma, L. W. Yap, W. L. Cheng, *Small* **2015**, *11*, 1886.
[26] Y. Zhang, R. Howver, B. Gogoi, N. Yazdi, *Solid-State Sensors* **2011**, *6*, 112.
[27] G. Schwartz, B. C. K. Tee, J. G. Mei, A. L. Appleton, D. H. Kim, H. L. Wang, Z. N. Bao, *Nat. Commun.* **2013**, *4*, 1859.
[28] H. K. Lee, S. I. Chang, E. Yoon, *J. Microelectromech. Syst.* **2006**, *15*, 1681.
[29] L. Viry, A. Levi, M. Totaro, A. Mondini, V. Mattoli, B. Mazzolai, L. Beccai, *Adv. Mater.* **2014**, *26*, 2659.
[30] M. Y. Cheng, X. H. Huang, C. W. Ma, Y. J. Yang, *J. Micromech. Microeng.* **2009**, *19*, 11500.
[31] C. Metzger, E. Fleisch, J. Meyer, M. Dansachmuller, I. Graz, M. Kaltenbrunner, C. Keplinger, R. Schwodiauer, S. Bauer, *Appl. Phys. Lett.* **2008**, *S92*, 01350601.

Received: March 6, 2016
Revised: May 2, 2016
Published online: